Acta of Bioengineering and Biomechanics
Vol. 14, No. 3, 2012

Original paper
DOI: 10.5277/abb120305

Application of muscle model to the musculoskeletal modeling

WIKTORIA WOJNICZ*, EDMUND WITTBRODT

Mechanics and Mechatronics Department, Mechanical Engineering Faculty, Gdańsk University of Technology, Gdańsk, Poland.

The purpose of this paper is to investigate new fusiform muscle models. Each of these models treats a muscle as a system composed of parts characterized by different mechanical properties. These models explain the influence of differences in the stiffness of lateral parts and the degree of muscle model discretization. Each muscle model is described by a system of differential equations and a single integro-differential equation. Responses of fifty-four muscle model forms are examined using a complex exertion composed of three types: eccentric-concentric exertion, isokinetic-isometric exertion and step exertion.

Key words: *muscle, modeling, differential equations system, integro-differential equation*

1. Introduction

Human locomotive apparatus consists of skeletal system (passive part) and striated skeletal muscle system (active part). The study of a muscle system in a living body is a difficult problem that can only be realized by using very specific measurement techniques [1]. This is why methods of mathematical modeling are often used to investigate this problem.

From the mechanical point of view, the system of muscles acting at a given human joint is a redundant system. Therefore, using only dynamic equations of motion will not provide a unique estimation of muscles contribution to a given joint movement. Sometimes the problem of muscles share estimation is solved as an inverse dynamic task using an optimization technique. This method does not require an application of precise physiological cause-and-effect relationships in a real muscle system but the optimization criterion still needs to be justified.

In order to obtain real muscles share estimation without using an optimization technique, a new mechanical model of fusiform muscle has been created and described in [2]–[4]. In this paper new types of this model are presented. These models have various stiffnesses of lateral parts and various degrees of muscle model discretization. Investigated here are the cases in which these models can be applied.

According to the rheological model presented in figure 1, a muscle is treated as a system composed of parts with different mechanical properties. This system is described as serially linked mass-damping-elastic parts and it simulates the influence of contractile non-stiff belly parts (active parts) and non-contractile stiff tendons (passive parts). The method of identification of muscle model mechanical properties is presented in detail in [4]. This muscle model confirms that muscle proximal force and muscle distal force are different [5]. Moreover, this model may be used to simulate the atypical behavior of a real muscle observed in practice, e.g., a force drop occurring at the start of isometric exertion followed by a shortening of the muscle [6]–[9].

A Hill-type muscle model is often used in muscle biomechanics [10]. This model treats the muscle as a whole, ignoring the fact that the belly is composed of several parts with different mechanical properties.

* Corresponding author: Wiktoria Wojnicz, Mechanics and Mechatronics Department, Mechanical Engineering Faculty, Gdańsk University of Technology, ul. G. Narutowicza 11/12, 80-233 Gdańsk, Poland. Tel.: +48 58 347 29 29, fax: +48 58 347 21 51, e-mail: wiktoria.wojnicz@pg.gda.pl

Received: December 31th, 2011
Accepted for publication: June 4th, 2012

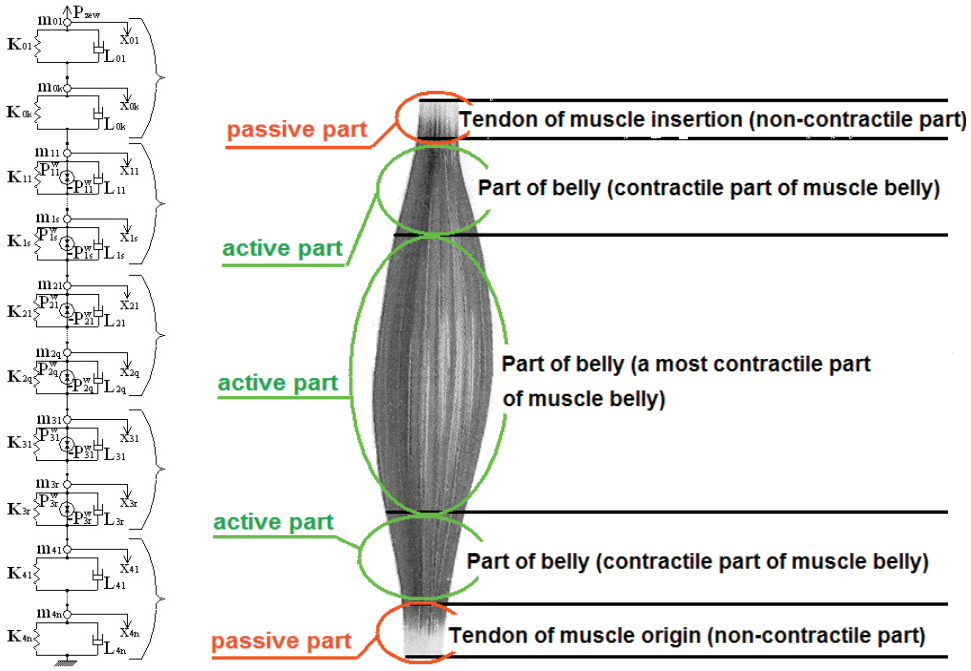

a) b)

Fig. 1: a) Rheological model of fusiform *i*-th muscle (Kj_i – stiffness coefficient of the *j*-th elastic element; L_{j_i} – damping coefficient of the *j*-th viscous element; m_{j_i} – mass of the *j*-th element; $P^{w}_{j\_i}(t)$ – internal force of the *j*-th forcible element; x_{ji} – displacement of the *j*-th point located on the *i*-th muscle surface; P_{zew} – external force); b) Physiological construction of fusiform muscle

This model usually describes the interaction of only one tendon and belly, and does not take into account how the muscle force is transmitted to the passive part of locomotive apparatus (the force is delivered from the belly through the belly-tendon connection and tendons). The Hill-type muscle model has two disadvantages. It cannot explain: 1) certain phenomena observed in a real muscle, e.g., the aforementioned force drop phenomenon; and 2) why the muscle proximal force and distal force are different. That is why, using the Hill-type muscle model as a base model, the authors of this paper have developed another method of muscle modeling to simulate more accurately a muscle behaviour.

2. Materials and methods

2.1. Types of muscle models

The influence of lateral part stiffness was examined by creating two types (stiffness type 1 and stiffness type 2) and nine modifications of each muscle model having the stiffness at their end parts: A1, A2, A3, B1, B2, B3, C1, C2, C3. In muscle model type 1, the stiffness coefficients are equal (figure 2a): K_A = 30000 N/m (simulating the influence of tendon tissue), K_B = 15000 N/m (simulating the influence of belly-tendon connection) and K_C = 5000 N/m (simulating the influence of belly tissue). In muscle model type 2, stiffness coefficients are equal (figure 2b): K_{A_1} = 4286 N/m, K_{B_1} = 3750 N/m and K_{C_1} = 2500 N/m. Each of the coefficients K_{A_1}, K_{B_1}, K_{C_1} describes the serial connection of the insertion tendon part with the upper belly part. The values of K_A, K_B, K_C, shown in figure 2b, are equal to the values described in figure 2a.

Using a part with stiffness K_A, one can simulate a muscle force delivered to the bone through a tendon. By applying a K_B stiffness part, one can simulate a muscle force delivered to the bone through the belly-tendon connection. Finally, by using the K_C stiffness part, one can simulate a muscle force delivered to the bone through the belly fibres only. On the other hand, using a part with stiffness K_{A_1} or K_{B_1} or K_{C_1}, one may simulate that muscle force delivered to the bone through the serial connection of the insertion tendon stiffness with the upper belly part stiffness.

The above-mentioned models can be used to describe the response of muscles: 1) with two tendons; 2) with only one tendon; 3) without tendons. External force $P_{zew}(t)$ only acts on the muscle insertion and depends on the time variable *t*.

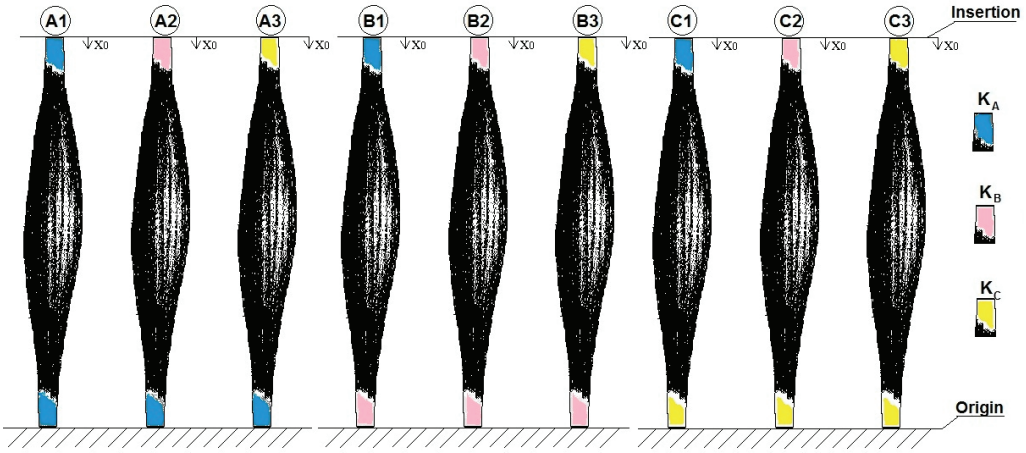

Fig. 2a. Modifications of muscle model (stiffness type 1)

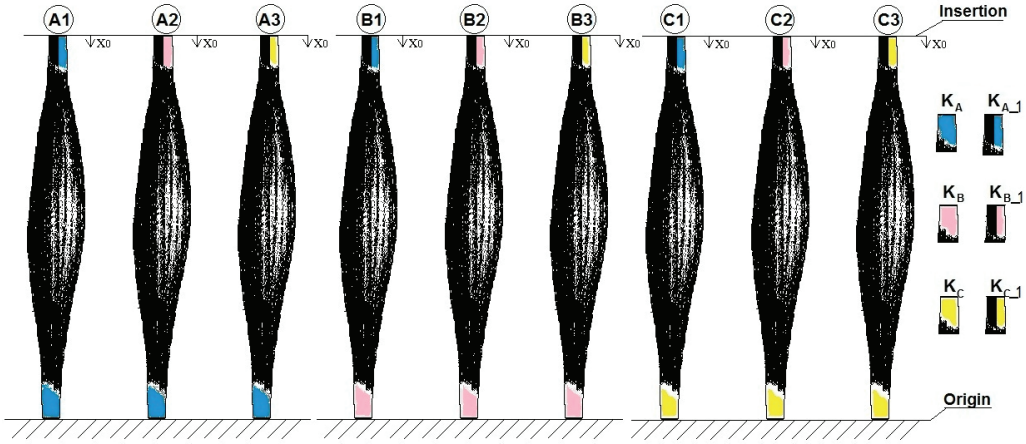

Fig. 2b. Modifications of muscle model (stiffness type 2)

Each *i*-th part of each muscle model (where $i = 0, 1, 2...$) is described by using the mass coefficient m_i, the stiffness coefficient K_i and the damping coefficient L_i. The contractile part of each muscle model additionally consists of the *j*-th forcible element which generates internal force $P_j^w(t)$.

The influence of the degree of muscle model discretization was examined by creating six muscle model types: 1) M1, a five-degree-of-freedom model (the stiffness type I is M1_I (figure 3, left side) and the stiffness type 2 is M1_II (figure 3, right side)); 2) M2, a three-degree-of-freedom model (the stiffness type 1 is M2_I (figure 5, left side) and the stiffness type 2 is M2_II (figure 5, right side)); 3) M3, a seven-degree-of-freedom model (the stiffness type 1 is M3_I (figure 4, left side) and the stiffness type 2 is M3_II (figure 4, right side)). The stiffness type 1 treats the muscle as a system composed of contractile belly parts and two non-contractile tendon parts. The stiffness type 2 describes the muscle as a system consisting of contractile belly parts and only one origin tendon.

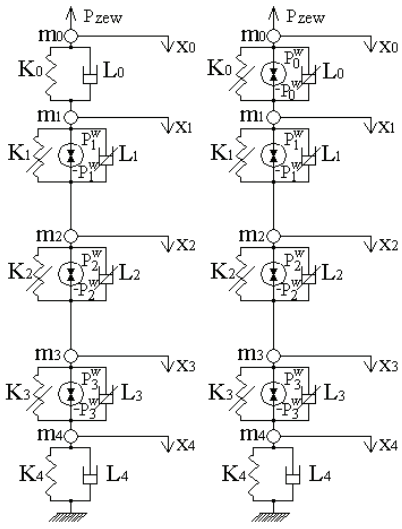

Fig. 3. Muscle model:
M1_I (left side) and M1_II (right side)

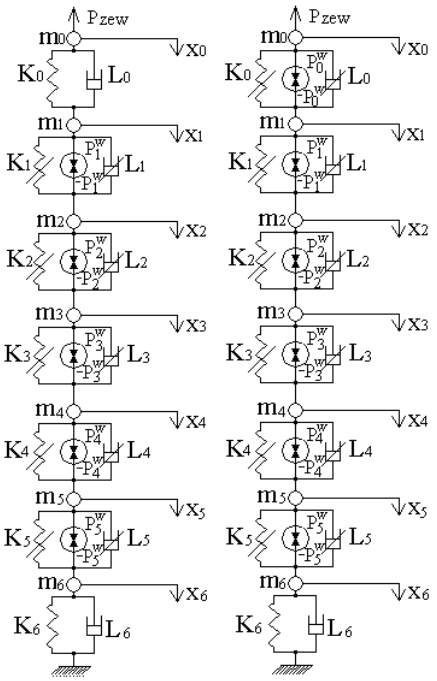

Fig. 4. Muscle model:
M3_I (left side) and M3_II (right side)

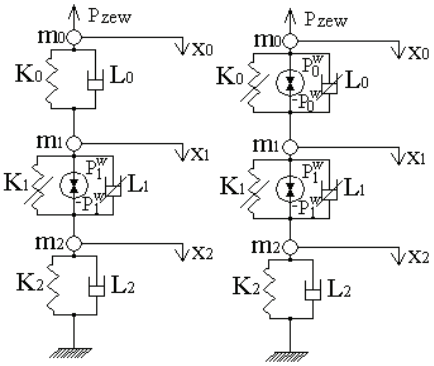

Fig. 5. Muscle model: M2_I (left side)
and M2_II (right side)

For the purpose of modelling the dynamics of a joint, each muscle model was reduced to the one-degree-of-freedom system. This reduction should be done towards the muscle insertion because the muscle force (called a contractile force) is directed from the insertion to the origin of muscle. The muscle contractile force is the difference between the active component and the passive component (the active component simulates the production of internal forces and the passive component simulates the resistance of the muscle).

The reduction is realized as the transformation of a *differential equation system DES* (describing model M1 (1), model M2 (3), model M3 (5)) to a single *integro-differential equation IDE* (describing model M1 (2), model M2 (4), model M3 (6)):

$$
\begin{aligned}
&m_0 \cdot \ddot{x}_0 + L_0 \cdot (\dot{x}_0 - \dot{x}_1) + K_0 \cdot (x_0 - x_1) = -P_{zew}(t) + P_0^w(t),\\
&m_1 \cdot \ddot{x}_1 + L_0 \cdot (\dot{x}_1 - \dot{x}_0) + K_0 \cdot (x_1 - x_0) + L_1 \cdot (\dot{x}_1 - \dot{x}_2) + K_1 \cdot (x_1 - x_2) = P_1^w(t) - P_0^w(t),\\
&m_2 \cdot \ddot{x}_2 + L_1 \cdot (\dot{x}_2 - \dot{x}_1) + K_1 \cdot (x_2 - x_1) + L_2 \cdot (\dot{x}_2 - \dot{x}_3) + K_2 \cdot (x_2 - x_3) = P_2^w(t) - P_1^w(t),\\
&m_3 \cdot \ddot{x}_3 + L_2 \cdot (\dot{x}_3 - \dot{x}_2) + K_2 \cdot (x_3 - x_2) + L_3 \cdot (\dot{x}_3 - \dot{x}_4) + K_3 \cdot (x_3 - x_4) = P_3^w(t) - P_2^w(t),\\
&m_4 \cdot \ddot{x}_4 + L_3 \cdot (\dot{x}_4 - \dot{x}_3) + K_3 \cdot (x_4 - x_3) + L_4 \cdot \dot{x}_4 + K_4 \cdot x_4 = -P_3^w(t),
\end{aligned}
\tag{1}
$$

$$
\begin{aligned}
&A_{2\_1} \cdot \ddot{x}_0(t) + A_{1\_1} \cdot \dot{x}_0(t) + A_{0\_1} \cdot x_0(t) + \int_0^t \left(\sum_{i=0}^{7} B_{i\_1} \cdot e^{s_{i\_1} \cdot (t-\tau)} \right) \cdot x_0(\tau)\, d\tau =\\
&\qquad = -P_{zew}(t) + \sum_{j=0}^{3} \left[\int_0^t \left(\sum_{i=0}^{3} C_{ij\_1} \cdot e^{s_{i\_1} \cdot (t-\tau)} \right) \cdot P_j^w(\tau)\, d\tau \right],
\end{aligned}
\tag{2}
$$

$$
\begin{aligned}
&m_0 \cdot \ddot{x}_0 + L_0 \cdot (\dot{x}_0 - \dot{x}_1) + K_0 \cdot (x_0 - x_1) = -P_{zew}(t) + P_0^w(t),\\
&m_1 \cdot \ddot{x}_1 + L_0 \cdot (\dot{x}_1 - \dot{x}_0) + K_0 \cdot (x_1 - x_0) + L_1 \cdot (\dot{x}_1 - \dot{x}_2) + K_1 \cdot (x_1 - x_2) = P_1^w(t) - P_0^w(t),\\
&m_2 \cdot \ddot{x}_2 + L_1 \cdot (\dot{x}_2 - \dot{x}_1) + K_1 \cdot (x_2 - x_1) + L_2 \cdot \dot{x}_2 + K_2 \cdot x_2 = -P_1^w(t),
\end{aligned}
\tag{3}
$$

$$A_{2\_2}\cdot\ddot{x}_0(t)+A_{1\_2}\cdot\dot{x}_0(t)+A_{0\_2}\cdot x_0(t)+\int_0^t\left(\sum_{i=0}^{3}B_{i\_2}\cdot e^{s_{i\_2}\cdot(t-\tau)}\right)\cdot x_0(\tau)\,d\tau=$$
$$=-P_{zew}(t)+\sum_{j=0}^{1}\left[\int_0^t\left(\sum_{i=0}^{3}C_{ij\_2}\cdot e^{s_{i\_2}\cdot(t-\tau)}\right)\cdot P_j^w(\tau)\,d\tau\right], \tag{4}$$

$$\begin{aligned}
&m_0\cdot\ddot{x}_0+L_0\cdot(\dot{x}_0-\dot{x}_1)+K_0\cdot(x_0-x_1)=-P_{zew}(t)+P_0^w(t),\\
&m_1\cdot\ddot{x}_1+L_0\cdot(\dot{x}_1-\dot{x}_0)+K_0\cdot(x_1-x_0)+L_1\cdot(\dot{x}_1-\dot{x}_2)+K_1\cdot(x_1-x_2)=P_1^w(t)-P_0^w(t),\\
&m_2\cdot\ddot{x}_2+L_1\cdot(\dot{x}_2-\dot{x}_1)+K_1\cdot(x_2-x_1)+L_2\cdot(\dot{x}_2-\dot{x}_3)+K_2\cdot(x_2-x_3)=P_2^w(t)-P_1^w(t),\\
&m_3\cdot\ddot{x}_3+L_2\cdot(\dot{x}_3-\dot{x}_2)+K_2\cdot(x_3-x_2)+L_3\cdot(\dot{x}_3-\dot{x}_4)+K_3\cdot(x_3-x_4)=P_3^w(t)-P_2^w(t),\\
&m_4\cdot\ddot{x}_4+L_3\cdot(\dot{x}_4-\dot{x}_3)+K_3\cdot(x_4-x_3)+L_4\cdot(\dot{x}_4-\dot{x}_5)+K_4\cdot(x_4-x_5)=-P_3^w(t)+P_4^w(t),\\
&m_5\cdot\ddot{x}_5+L_4\cdot(\dot{x}_5-\dot{x}_4)+K_4\cdot(x_5-x_4)+L_5\cdot(\dot{x}_5-\dot{x}_6)+K_5\cdot(x_5-x_6)=-P_4^w(t)+P_5^w(t),\\
&m_6\cdot\ddot{x}_6+L_5\cdot(\dot{x}_6-\dot{x}_5)+K_5\cdot(x_6-x_5)+L_6\cdot\dot{x}_6+K_6\cdot x_6=-P_5^w(t),
\end{aligned} \tag{5}$$

$$A_{2\_3}\cdot\ddot{x}_0(t)+A_{1\_3}\cdot\dot{x}_0(t)+A_{0\_3}\cdot x_0(t)+\int_0^t\left(\sum_{i=0}^{11}B_{i\_3}\cdot e^{s_{i\_3}\cdot(t-\tau)}\right)\cdot x_0(\tau)\,d\tau=$$
$$=-P_{zew}(t)+\sum_{j=0}^{5}\left[\int_0^t\left(\sum_{i=0}^{11}C_{ij\_3}\cdot e^{s_{i\_3}\cdot(t-\tau)}\right)\cdot P_j^w(\tau)\,d\tau\right], \tag{6}$$

where:

$A_{0\_1}\div A_{2\_1}$, $B_{0\_1}\div B_{7\_1}$, $C_{0\ 0\_1}\div C_{7\ 0\_1}$, $C_{0\ 1\_1}\div C_{7\ 1\_1}$, $C_{0\ 2\_1}\div C_{7\ 2\_1}$, $C_{0\ 3\_1}\div C_{73\_1}$, $A_{0\_2}\div A_{2\_2}$, $B_{0\_2}\div B_{3\_2}$, $C_{0\ 0\_2}\div C_{3\ 0\_2}$, $C_{0\ 1\_2}\div C_{3\ 1\_2}$, $A_{0\_3}\div A_{2\_3}$, $B_{0\_1}\div B_{11\_3}$, $C_{0\ 0\_3}\div C_{11\ 0\_3}$, $C_{0\ 1\_3}\div C_{11\ 1\_3}$, $C_{0\ 2\_3}\div C_{11\ 2\_3}$, $C_{0\ 3\_3}\div C_{11\ 3\_3}$, $C_{0\ 4\_3}\div C_{11\ 4\_3}$, $C_{0\ 5\_3}\div C_{11\ 5\_3}$ – coefficients depending on the mass coefficients, stiffness coefficients and damping coefficients;

$s_{0\_1}\div s_{7\_1}$, $s_{0\_2}\div s_{3\_1}$, $s_{0\_3}\div s_{11\_1}$ – eigenvalues depending on the mass coefficients, stiffness coefficients and damping coefficients;

τ – time variable used in the integral function.

The coefficients of *IDE* were calculated by using Symbolic Toolbox of Matlab.

It worth noticing that in stiffness type 1 the internal force $P_0^w(t)$ is neglected.

3. Results

The responses of 54 forms (9-modifications · 6-muscle-model-types) were examined using a complex exertion composed of: eccentric-concentric exertion, isokinetic-isometric exertion and step exertion. Each form was calculated by using *DES* and *IDE*.

The data for the numerical simulations were as follows: belly length 0.211986 m, a musculotendon

Table 1. Mass coefficients

m_i	Model type					
	M1_I [kg]	M1_II [kg]	M2_I [kg]	M2_II [kg]	M3_I [kg]	M3_II [kg]
m_0	0.000816	0.003895	0.000816	0.003895	0.000816	0.001925
m_1	0.017712	0.014633	0.143700	0.140621	0.004386	0.001971
m_2	0.108275	0.108275	0.000816	0.000816	0.025665	0.014633
m_3	0.017712	0.017712	x	x	0.0819927	0.108275
m_4	0.000816	0.000816	x	x	0.025665	0.014633
m_5	x	x	x	x	0.004386	0.003079
m_6	x	x	x	x	0.000816	0.000816

length 0.328 m, tendon diameter 4 mm, mass coefficients as described in table 1 (calculated according to the method presented in [2], stiffness coefficients of belly parts as described in table 2, each i-th damping coefficient L_i equalled $0.1 \cdot K_i$.

Table 2. Stiffness coefficients of belly parts

K_i	*Model type*					
	M1_I [N/m]	M1_II [N/m]	M2_I [N/m]	M2_II [N/m]	M3_I [N/m]	M3_II [N/m]
K_1	5000	5000	937.5	937.5	5000	5000
K_2	1500	1500	x	x	3250	3250
K_3	5000	5000	x	x	1500	1500
K_4	x	x	x	x	3250	3250
K_5	x	x	x	x	5000	5000

From the mechanical point of view, the connection of stiff tendon parts with flexible (non-stiff) belly parts is a system composed of very different eigenvalues [11]. That is why one needs to use specific numerical methods for numerical simulations.

Taking into account the relation of the maximum real part of *DES* eigenvalue to the minimum real part of *DES* eigenvalue, the above-mentioned model types were divided into three variants: the high stiffness model, the medium stiffness model and the low stiffness model (table 3). The values of M1_I model are presented in table 4.

Table 3. Muscle type modification

Type of modification	$\frac{\max(\text{real(eigenvalue)})}{\min(\text{real(eigenvalue)})}$
The high stiffness model (for A1, A2, A3 modifications)	[378 900; 433 000]
The medium stiffness model (for B1, B2, B3 modifications)	[195 200; 251 000]
The low stiffness model (for C1, C2, C3 modifications)	[72 730; 133 000]

Table 4. Eigenvalues of M1_I model

DES [s^{-1}]	IDE [s^{-1}]
–4291130.299	–4291130.299
–3845254.680	–198270.537
–33832.017	–33044.889
–30896.183	–4894.026
–853.611	–10.020
–10.118	$-10.002 + 0.002i$
$-10.013 + 0.012$	$-10.002 - 0.002i$
$-10.013 - 0.012i$	–9.998
$-9.989 + 0.011i$	
$-9.989 - 0.011i$	

The eccentric exertion was caused by external force of 10 N. The next concentric exertion was caused by internal forces generated in the active parts of the muscle belly. In all the simulations it was assumed that a given muscle volume could generate an internal force of 20 N. The forcible element of a belly part can generate a force proportional to the mass coefficient of this part. The muscle model response is described by muscle insertion displacements and several points located on the muscle surface (each M1 stiffness type has five points (figure 6), each M2 stiffness type has three points (figure 7) and each M3 stiffness type has seven points (figure 8)).

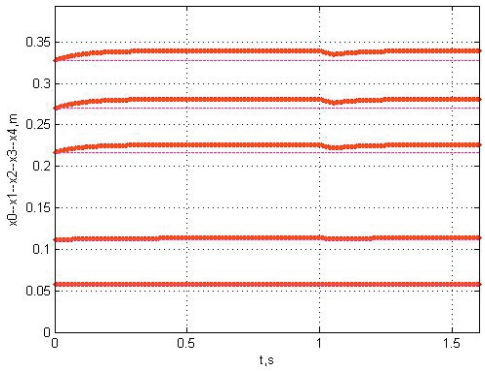

Fig. 6. Displacements of the M1_I_A1 model

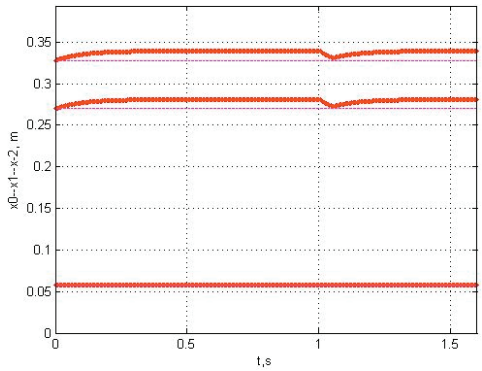

Fig. 7. Displacements of the M2_I_A1 model

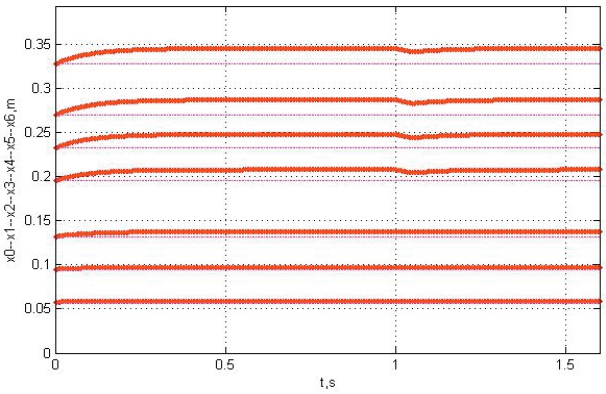

Fig. 8. Displacements of the M3_I_A1 model

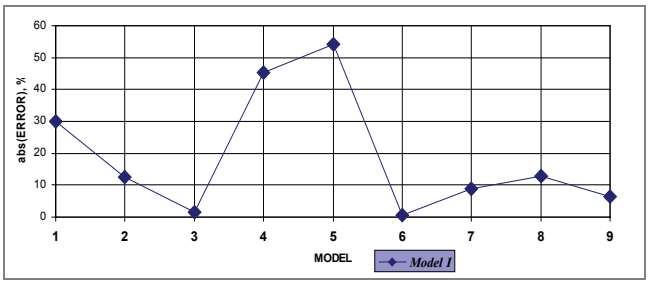

Fig. 9. Relative errors of the M1_I model, where no. 1 is A1, no. 2 is A2, no. 3 is A3, no. 4 is B1, no. 5 is B2, no. 6 is B3, no. 7 is C1, no. 8 is C2, no. 9 is C3 modification shown in fig. 2a

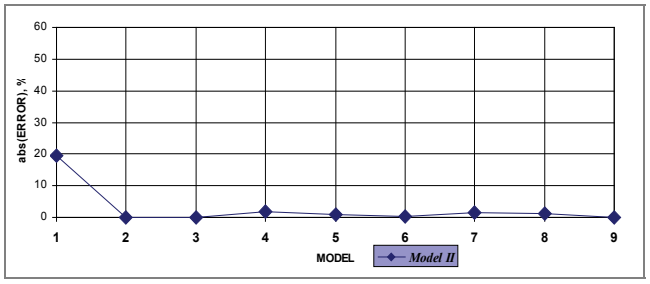

Fig. 10. Relative errors of the M1_II model, where no. 1 is A1, no. 2 is A2, no. 3 is A3, no. 4 is B1, no. 5 is B2, no. 6 is B3, no. 7 is C1, no. 8 is C2, no. 9 is C3 modification shown in fig. 2b

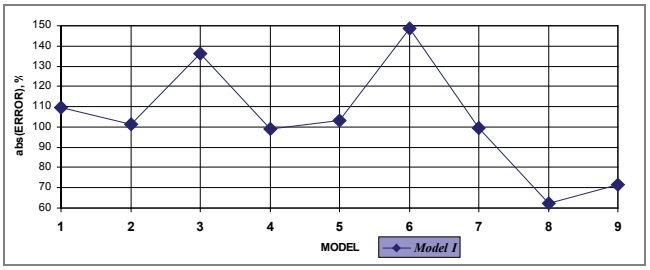

Fig. 11. Relative errors of the M3_I model, where no. 1 is A1, no. 2 is A2, no. 3 is A3, no. 4 is B1, no. 5 is B2, no. 6 is B3, no. 7 is C1, no. 8 is C2, no. 9 is C3 modification shown in fig. 2a

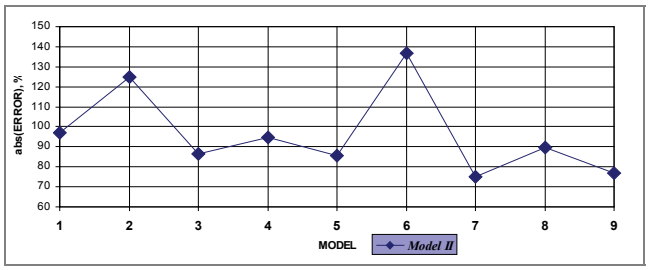

Fig. 12. Relative errors of the M3_II model, where no. 1 is A1, no. 2 is A2, no. 3 is A3, no. 4 is B1, no. 5 is B2, no. 6 is B3, no. 7 is C1, no. 8 is C2, no. 9 is C3 modification shown in fig. 2b

A comparison of *DES* response and *IDE* response was made in a static state by calculating the relative error of *IDE* model (i.e., error [%] = (*DES* – *IDE*)/ *DES*·100%). Three modifications of M1_I model (A1, B1, B2) have a large error (figure 9) (the high and medium stiffness models) but this error diminished as the stiffness decreased. Therefore, only A1 modification of the M1_II has a large error (figure 10).

Two stiffness types of model M2 have a very low error, 10^{-9}%.

Two stiffness types of model M3 have a very large error (figures 11 and 12).

It is worth observing the shapes of the *DES* and *IDE* runs. The *IDE* run of M1_I_A1 model is similar to the *DES* run, although their insertion displacements differ in the static state (figures 13 and 14). On the other hand, the M1_II_A1 model *IDE* run is similar to the *DES* run in both states (figures 15 and 16). The *DES* runs and the *IDE* runs of two stiffness types M2 are identical (that is why they are not presented in this paper). Eight modifications of the M3_I model (A1, A2, A3, B1, B2, B3, C1, C2) have divergent *IDE* numerical results (but their *DES* results are convergent). Only the C3 modification of the M3_I model has a convergent *IDE* result (figures 17 and 18) (but it does not coincide with the *DES* result). All modifications of the M3_II model have *IDE* convergent results that do not coincide with the *DES* results (figures 19 and 20).

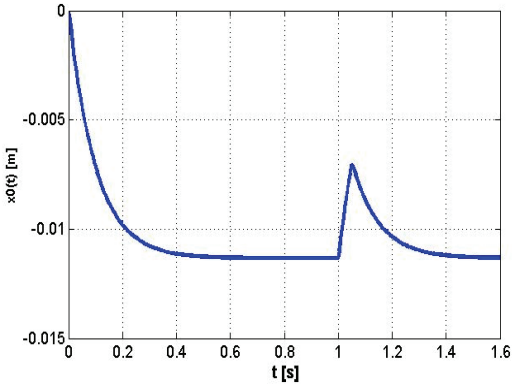

Fig. 13. DES results of M1_I_A1 model

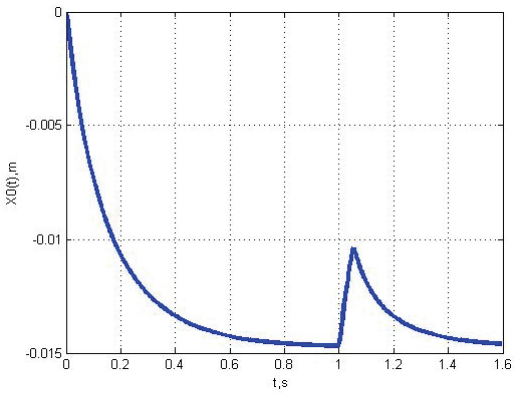

Fig. 14. IDE results of M1_I_A1 model

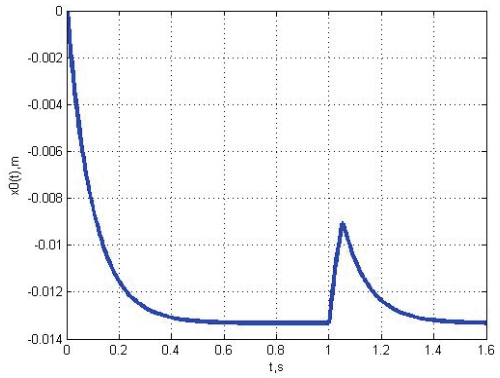

Fig. 15. DES results of M1_II_A1 model

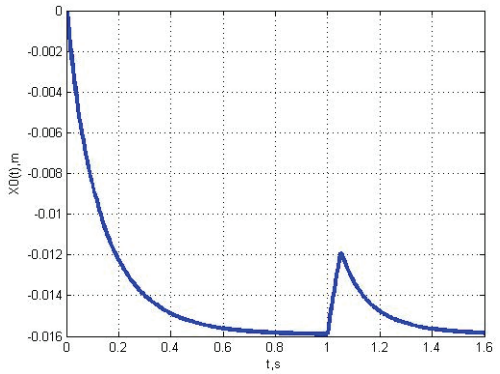

Fig. 16. IDE results of M1_II_A1 model

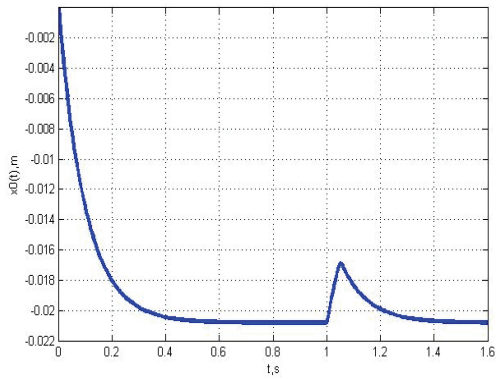

Fig. 17. DES results of M3_I_C3 model

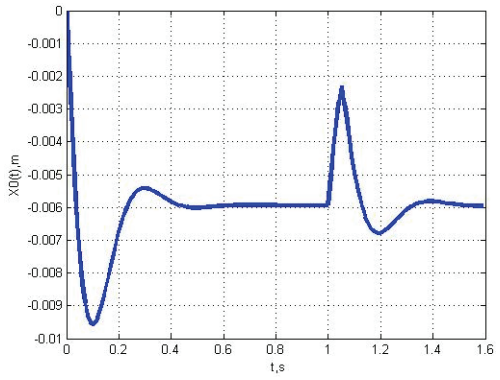

Fig. 18. IDE results of M3_I_C3 model

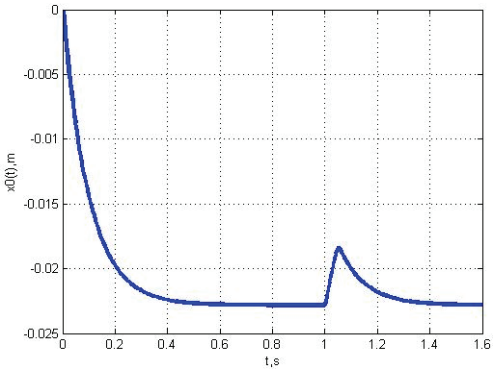

Fig. 19. DES results of M3_II_C3 model

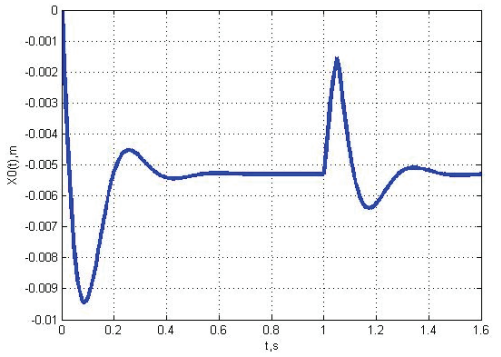

Fig. 20. IDE results of M3_II_C3 model

The *IDE* results of isokinetic-isometric exertion simulations are presented in figures 21–26, while the *IDE* step exertion simulation results are presented in figures 27–32. The value P_{kurcz} is a contractile force which is equal to the external force as $P_{kurcz} = -P_{zew}$. By analyzing these results one can see that the first rapid force change occurs at the start of isokinetic exertion (figures 21–26) and step exertion (figures 27–32). The second force change occurs at the start of isometric exertion (figures 21–26). The first sudden change is caused by the initial conditions of the model (both the contractile force and the insertion displacement equal

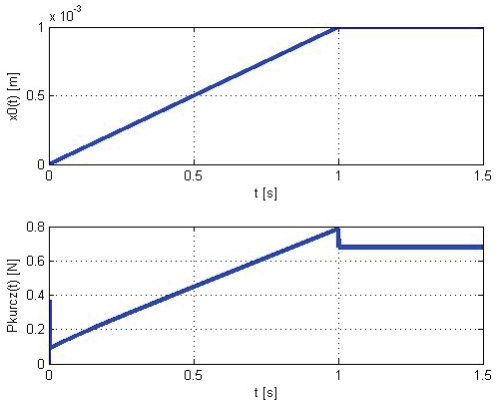

Fig. 21. IDE results of the M1_I_A1 model

zero). The second force change is caused by the rapid change of insertion displacement velocity, as the isokinetic exertion turns into isometric insertion. In five models (M1_I_A1, M2_I_A1, M1_II_A1, M2_II_A1, M3_II_A1) this change is a force enhancement, thus in only one model (M3_I_A1 which is a high stiffness model) this change is a force drop.

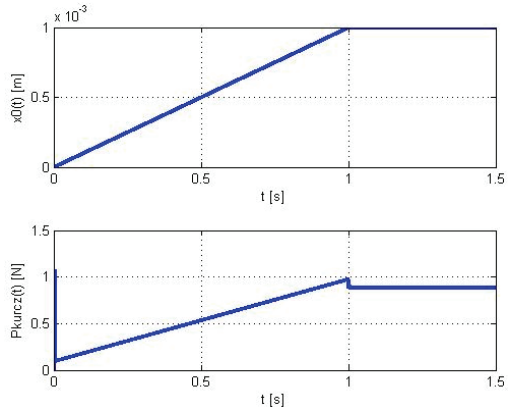

Fig. 22. IDE results of the M2_I_A1 model

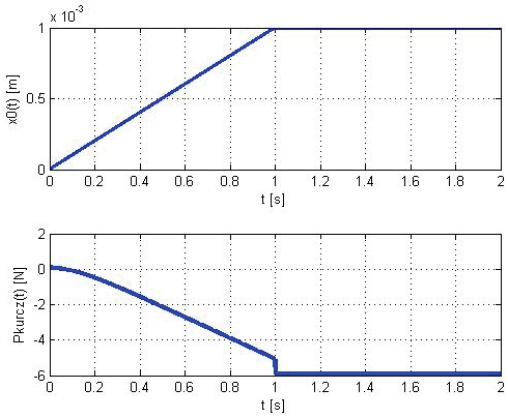

Fig. 23. IDE results of the M3_I_A1 model

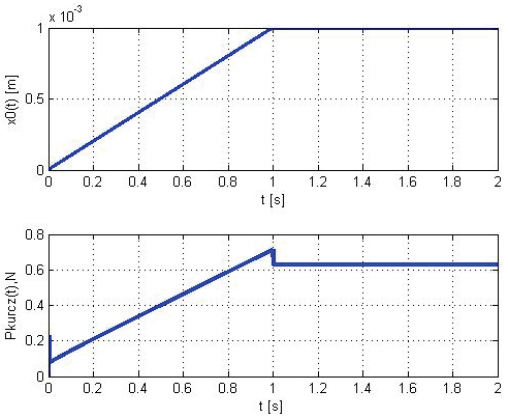

Fig. 24. IDE results of the M1_II_A1 model

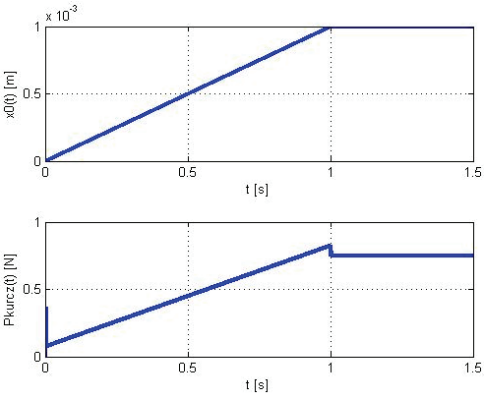

Fig. 25. IDE results of the M2_II_A1 model

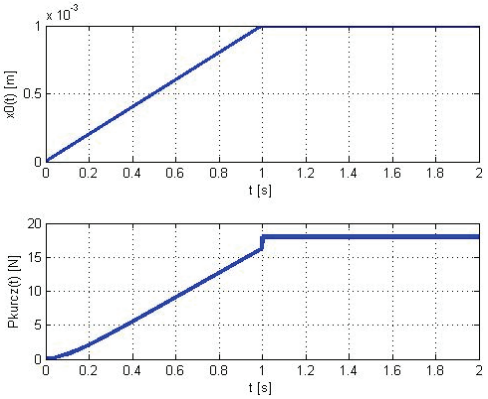

Fig. 26. IDE results of the M3_II_A1 model

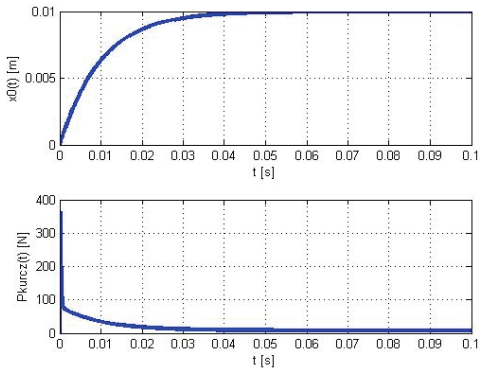

Fig. 27. IDE results of the M1_I_A1 model

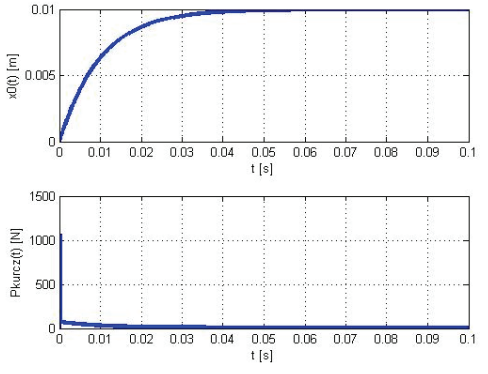

Fig. 28. IDE results of the M2_I_A1 model

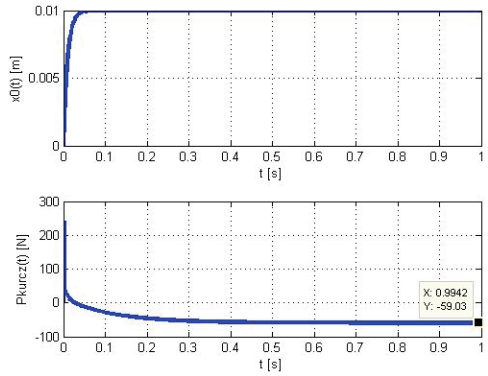

Fig. 29. IDE results of the M3_I_A1 model

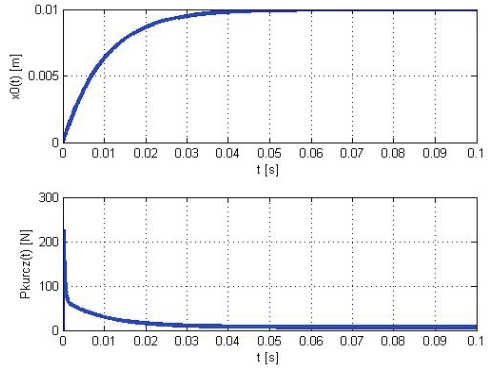

Fig. 30. IDE results of the M1_II_A1 model

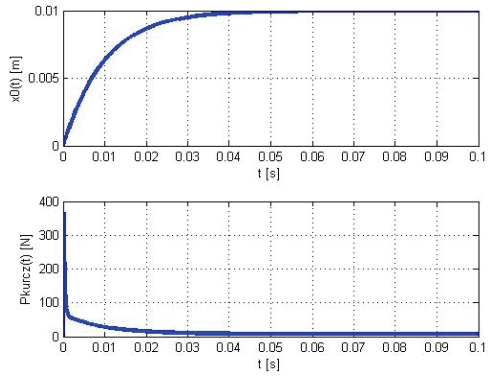

Fig. 31. IDE results of the M2_II_A1 model

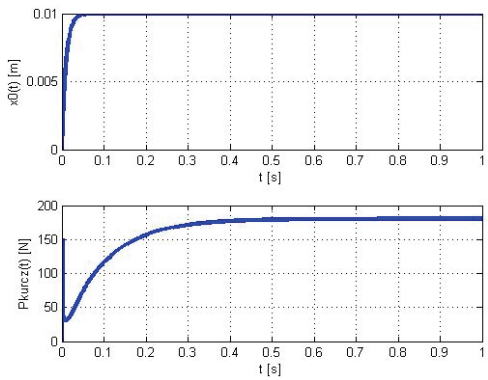

Fig. 32. IDE results of the M3_II_A1 model

4. Discussion

Analysis of the results shows that by increasing the degree of model discretization (as in the Finite Element Method), a higher accuracy of model simulation may be obtained. However, one should remember that results of system having parts with different mechanical properties may contain numerical errors caused by computer rounding (i.e., truncation). These errors could be diminished by adding numerical damping (but this method requires a lot of tests). It is worth noticing that the errors caused by computer rounding are significant for a system having a high and medium stiffness as well as several degrees of freedom.

The M2 models (stiffness type 1 and stiffness type 2) are the simplest and their *DES* and *IDE* results are convergent (the relative error is 10^{-9}%). These two models can be used to describe short muscles with short tendons or the ones directly fixed to bones by lateral belly parts (for example, facial muscles). However, these models cannot be used to simulate a long muscle because these do not describe in what manner internal forces are distributed in belly parts.

The M1 model and the M3 model can be used to describe long fusiform muscles by giving information about the manner of internal force distribution in exerted muscle parts. However, one should bear in mind that these models have different *DES* and *IDE* results, especially in the high stiffness model.

Using a system of serially linked parts having different mechanical properties, it is possible to simulate a muscle without tendons, with one tendon only, with two tendons or with different belly part properties. This method also allows us to model: 1) the force drop phenomenon occurring at the start of isometric exertion after the shortening of the muscle; 2) the force enhancement occurring at the start of isometric exertion after the lengthening of the muscle. These phenomena occur in a mechanical system composed of stiff and flexible parts serially linked.

Acknowledgements

The numerical simulations were performed using computers of "Centrum Informatyczne Trójmiejskiej Akademickiej Sieci Komputerowej" in Gdańsk, Poland.

This work was accomplished under the research project No. 3156/B/T02/2010/39 and was financed by the Polish Ministry of Science and Higher Education.

References

[1] de LUCA C.J., *The use of surface electromyography in biomechanics*, Journal of Applied Biomechanics, 1997, 13, 135–163.

[2] WOJNICZ W., *Modelowanie i symulacja zachowania zespołu mięśni szkieletowych układu ramię–przedramię*, PhD Thesis, 2009, Technical University of Łódź, Poland.

[3] WOJNICZ W., WITTBRODT E., *Analysis of muscles behaviour*. Part I – *The computational model of muscle*, Acta of Bioengineering and Biomechanics, 2009, No. 4, 15–21.

[4] WOJNICZ W., WITTBRODT E., *Analysis of muscles behaviour*. Part II – *The computational model of muscles group acting on the elbow joint*, Acta of Bioengineering and Biomechanics, 2010, No. 1, 3–10.

[5] YUCESOY C.A., KOOPMAN B.H.F.J.M., HUIJING P.A., GROOTENBOER H.J., *Three dimensional finite element modeling of skeletal muscle using a two-domain approach: linked fiber-matrix mesh model*, Journal of Biomechanics, 2002, 35, 1253–1262.

[6] BULLIMORE S.R., LEONARD T.R., RASSIER D.E., HERZOG W., *History-dependence of isometric muscle force: Effect of prior stretch or shortening amplitude*, Journal of Biomechanics, 2007, 40, 1518–1524.

[7] HERZOG W., *History dependence of force production in skeletal muscle: a proposal for mechanisms*, Journal of Electromyography and Kinesiology, 1998, 8, 111–117.

[8] MCGOWAN C.P., NEPTUNE R., HERZOG W., *A phenomenological model and validation of shortening-induced force depression during muscle contractions*, Journal of Biomechanics, 2010, 43, 449–454.

[9] ROUSANOGLOU E.N., OSKOUEI A.E., HERZOG W., *Force depression following muscle shortening in sub-maximal voluntary contractions of human adductor pollicis*. Journal of Biomechanics, 2007, 40, 1–8.

[10] HUIJING P.A., *Parameter interdependence and success of skeletal muscle modeling*, Human Movement Science, 1995, 14, 443–486.

[11] WOJNICZ W., WITTBRODT E., *Chosen aspects of muscle biomechanics*. *Dynamical Systems, Nonlinear Dynamics and Control*, The 11-th Conference on Dynamical Systems, Theory and Applications, J. Awrejcewicz et al. (ed.), 2011, 263–268.